Available online at www.sciencedirect.com
ScienceDirect
Infrared Physics & Technology 50 (2007) 253–259
INFRARED PHYSICS & TECHNOLOGY
www.elsevier.com/locate/infrared

LWIR/SWIR switchable two color device based on InP/InGaAs integrated HBT/QWIP

N. Cohen [a,b,*], R. Gardi [a], G. Sarusi [b], A. Sa'ar [a], M. Byloos [c], A. Bezinger [c], A.J. SpringThorpe [c], H.C. Liu [c]

[a] *Racah Institute of Physics and the Center for Nanoscience and Nanotechnology, The Hebrew University of Jerusalem, Jerusalem 91904, Israel*
[b] *ELOP Electrooptic Industries Ltd., Rehovot 76111, Israel*
[c] *Institute for Microstructural Sciences, National Research Council, Ottawa, Canada K1A 0R6*

Available online 13 November 2006

Abstract

A novel two color infrared (IR) device that allows fast electrical switching between the short wavelength IR (SWIR) band (0.9–1.6 μm) and the long wavelength IR (LWIR) band (8–12 μm) is presented. The integrated sensor is based on MOCVD grown, lattice matched (to InP substrate) epilayers of InGaAs/InP and consists of two, monolithically integrated sections of heterojunction bipolar transistor (HBT) and quantum well infrared photodetector (QWIP).
© 2006 Elsevier B.V. All rights reserved.

Keywords: QWIP; See-spot; HBT; Two color; SWIR; InP

1. Introduction

The increasing demand for future generations of infrared (IR) thermal imaging systems have led to an extensive research aimed at developing multi-spectral IR imaging systems. Usually there is a gap between the technological capabilities and the operational needs. In some cases the multi-spectral imaging technology provides a solution to an unknown application while in other cases the application is well known but the technology is not well established. During the past few years we have developed a technology that was aimed a-priory for a family of applications that integrate thermal imaging with near-IR imaging. The first generation of the integrated device, it's concept and performances were published elsewhere [1]. This two color, see-spot imager was based on the GaAs/InGaAs material system and includes LWIR imager combined with a Nd:YAG laser spot imager. A two dimensional array (320×256 elements) was fabricated from that device. The array was flip chip bonded to a commercial ROIC (Indigo 9705) and was integrated in an imaging system. This imager shows excellent performances to be published elsewhere.

In this work we demonstrate a second generation device that is based on similar concepts with improved performances. The imager is based on the lattice matched InP/InGaAs material system that allows an extended near-IR (NIR) imaging capabilities to become a true SWIR imager that is sensitive up to 1.6 μm. In addition, the second generation imager is based on bound-to-free optical transitions, as opposed to bound-to-bound transitions in the previous (see-spot) imager and therefore, we obtained higher NIR sensitivity. Another advantage of this device is the expected faster time response due to the higher mobility of the hot carriers which makes the device suitable for very short laser pulses applications.

* Corresponding author. Address: Racah Institute of Physics and the Center for Nanoscience and Nanotechnology, The Hebrew University of Jerusalem, Jerusalem 91904, Israel. Tel.: +972 8 9386693; fax: +972 8 9386714.
E-mail address: el05159@elop.co.il (N. Cohen).

1350-4495/$ - see front matter © 2006 Elsevier B.V. All rights reserved.
doi:10.1016/j.infrared.2006.10.022

2. Device concept

The concept of the device is similar to the first generation see-spot device [1]. It contains two portions; the first is a floating base heterojunction bipolar transistor (HBT) that functions as a SWIR phototransistor and a second portion of a quantum well IR photodetector (QWIP) that functions as an LWIR sensor. The two portions of the device are monolithically integrated in series with only two contact terminals defined at the edges of the device. When the device is biased below the breakdown voltage, all the applied voltage is dropped across the HBT (since the QWIP impedance is much smaller than that of the HBT). At this range of bias voltages the device functions as a high gain SWIR detector where the QWIP neither contributes to the photocurrent nor to the dark current. When the bias voltage is raised the HBT is switched to the predesigned punch through breakdown mode of operation. In this range the HBT is shortcut and the QWIP is activated. In this range of high bias voltages the integrated device functions as a LWIR detector.

The punch through breakdown mechanism is reversible, fast and characterized by low-noise. Therefore, it can be used for switching between the two spectral bands. It should be emphasized that the high and low bias voltage mode are at the same polarity, thus making the device compatible with commercially available ROIC.

3. HBT characterization

Based on results from the previous see-spot GaAs/InGaAs structure [1], we have designed, grow, fabricate and characterize a second generation device that is based on the lattice matched InGaAs/InP material system. At first, in order to demonstrate the operation of the punch-through HBT, we have fabricated and characterized a stand-alone HBT structure. The structure was grown by MOCVD on top of semi-insulating InP substrate and consists of 100 nm InP buffer layer, InP contacts, InGaAs collector and base and InP emitter (see Fig. 1 for details). All n-type layers were doped with Si while p-layers with Zn.

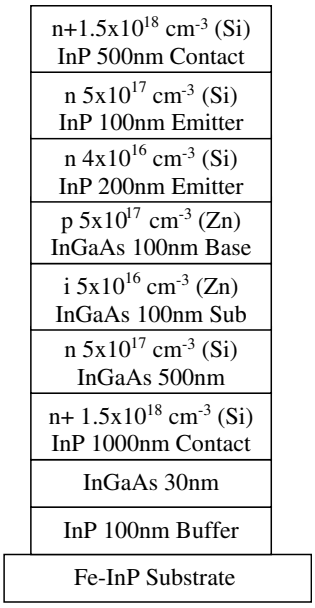

Fig. 1. The HBT structure layers.

The measured dark current of the device at 77 K is shown in Fig. 2. As can be seen, at low bias voltages (up to ±1 V) the dark current is very low, of the order of

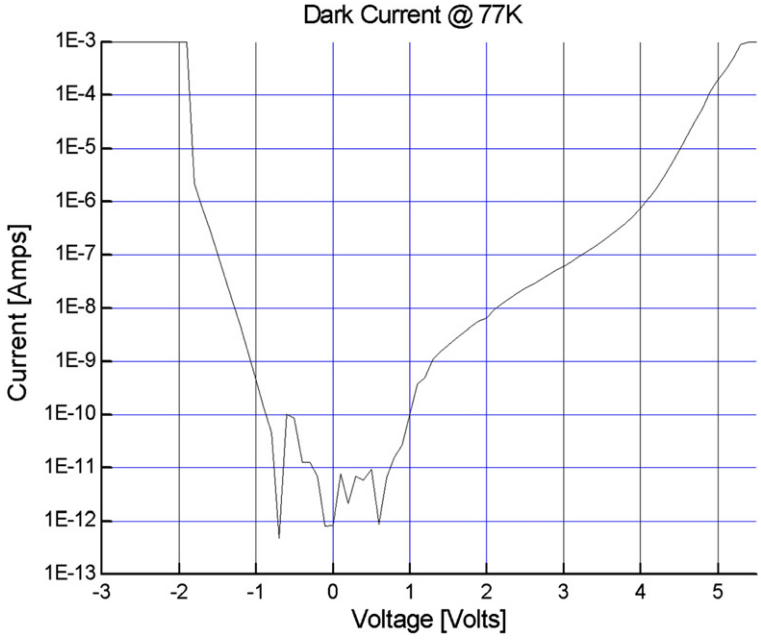

Fig. 2. HBT dark current at 77 K.

10^{-11} A. This low dark current of the device (below the punch-through breakdown voltage) indicates that the impedance of the HBT is much higher than the impedance of the QWIP. This would ensure that, in the integrated device, the bias voltage drops across the HBT and not across the QWIP (which has a typical impedance that is few orders of magnitude lower).

At higher bias voltages the diode breakdown can be seen. We notice that the breakdown voltage (at about −1.8 V) can be tuned by appropriate design of the structural parameters (such as width and the doping of the base and emitter layers). Later on we will show that the breakdown of the HBT is due to punch-through process and not due to avalanche mechanism. As an empirical rule it has been claimed that avalanche breakdown occurs at bias voltage level of $6*Eg/q$ [2] which, in our case, should take place at a voltage of ~4.5 V.

Next, we have measured the *I–V* characteristics of the devices under variable illumination level. The *I–V* characteristics under increasing intensity level at a wavelength of 1540 nm are shown in Fig. 3. The illumination source is Halogen (TQH) lamp focused into the entrance port of a 1/4 m monochromator for monochromatic illumination.

As can be seen from Fig. 3, the device operates as SWIR detector at bias voltages below the breakdown point. The absolute response of the device has been measured at 1064 nm using a calibrated, diode pumped cw Nd:YAG laser. In Fig. 4 we show the absolute response at 77 K and a bias voltage of −1 V, vs. the laser power at the detector plain.

Notice the very high response, up to 250 A/W, at relatively low laser intensities. The high responsivity of the device is due to the inherent gain of the HBT where the exponential behavior is related to the increasing photoconductive gain with the increasing base-current at higher photons flux. Notice that the photocurrent replaces the base current in our floating base HBT. Therefore, the transistor's gain (β), represents the photo-conductive gain that increases with the increasing base-current. Hence, the total optical gain, which is the product of the photo-conductive gain and the quantum efficiency [3], increases with the increasing photon flux.

The higher response of the InP/InGaAs device as compared to the GaAs/InGaAs HBT can be explained as follows. In our second generation InP/InGaAs HBT, the optical transitions generates free carriers in the transistor base while in the GaAs/InGaAs the optical transitions were in between bound states (bound to bound transitions) states in the sub-collector. Hence, every optical transition in our device generates a free carrier that charges the base as opposed to the previous device where the efficiency of the charging process was fairly poor [1]. In addition, the fact that we have used lattice-matched alloys does not impose limitations of the thickness of the active layer is another advantage relative to the previous device, which help to improve the quantum efficiency of the current device.

The absolute response of the device vs. bias voltage, up to −1 V, is shown in Fig. 5. As expected, the responsivity of the device increases with the increasing bias voltage. Operating the device at SWIR mode can be done under bias of up to the breakdown point, but as shown in Fig. 5, it could be operated at lower bias of about −1 V where the absolute response is sufficient, especially at high optical flux.

As was shown, the photoconductive gain of the device is very high. To verify that the origin of the gain does not related to avalanche mechanism, we have measured the

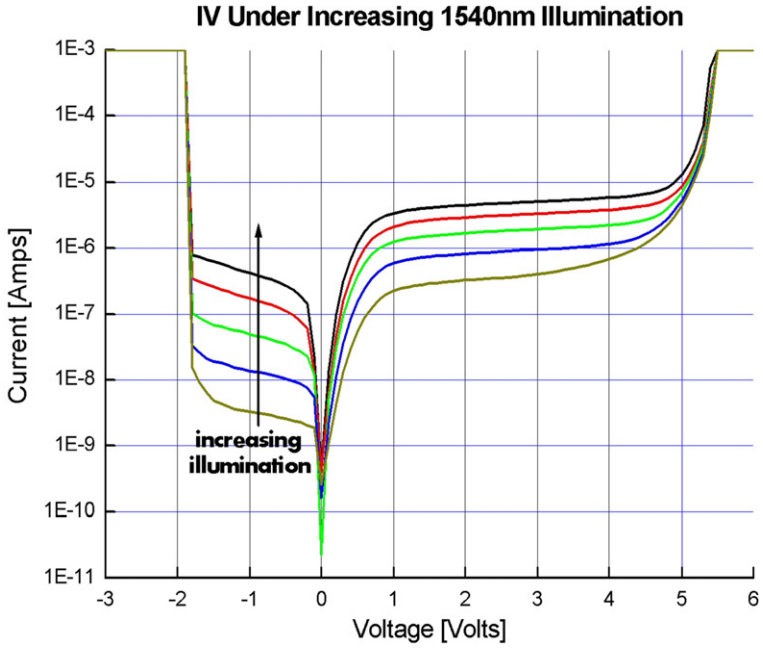

Fig. 3. *I–V* under 1540 nm increasing illumination.

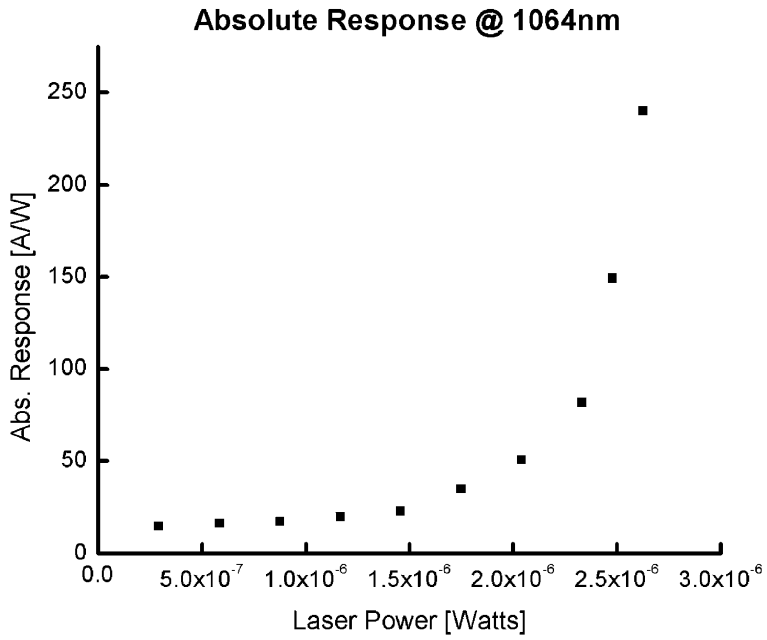

Fig. 4. Absolute response vs. YAG laser power.

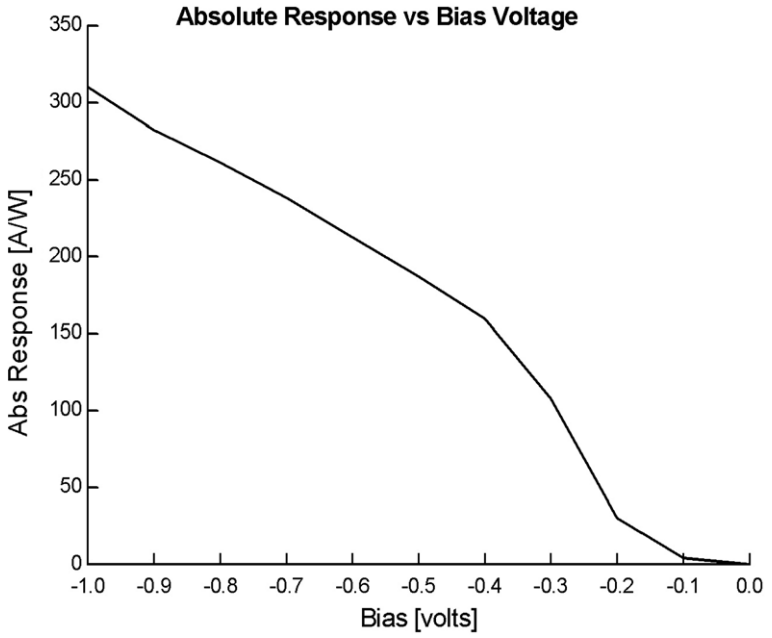

Fig. 5. The absolute response vs. bias voltage.

dependency of the breakdown voltage on temperature; see Fig. 6. As can be seen the breakdown voltage decreases with increasing temperature. It is well known that the avalanche process has a positive temperature coefficient, i.e., the breakdown voltage increases with increasing temperature. A simple explanation for the increase [2] is that hot carriers should lose their energy to optical phonons. Hence, since the mean free path (λ) decreases with temperature, the carriers should acquire sufficient energy to generate electron–hole pair. The negative temperature coefficient shown in Fig. 6 proves that no avalanche process involves in our device.

Furthermore, as shown in Fig. 3, the breakdown voltage is not affected by the optical flux. Campbel et al. [4] have shown that under avalanche conditions the breakdown voltage decreases with the increasing optical flux. This, again, proves that in our device the breakdown is not related to avalanche process.

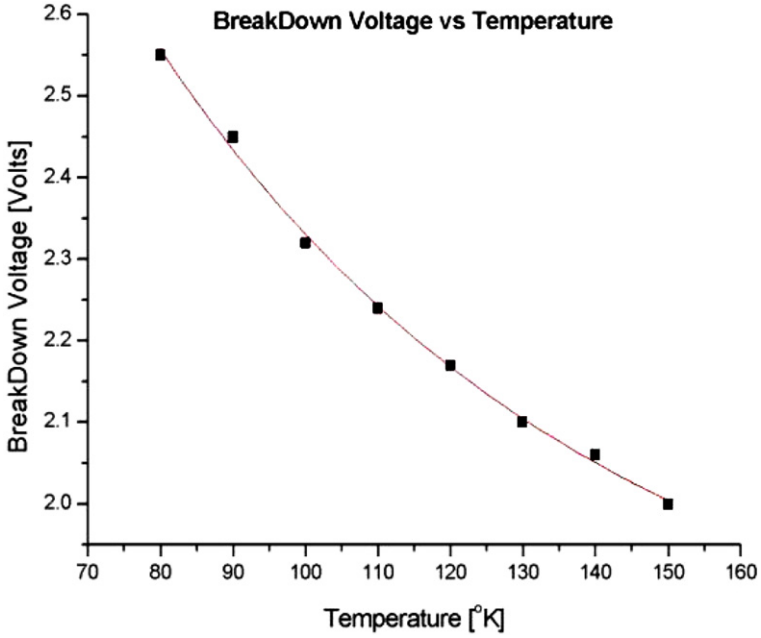

Fig. 6. Breakdown voltage vs. device temperature.

Another important parameter of the device is its bandwidth and time response as in many applications the device should respond to short laser pulses. In order to verify that the device is "fast" enough we have measured the device response to a 100 ns Nd:YAG laser pulses. In Fig. 7 we show the temporal response of device and compare it to the temporal response of a fast (1 ns) Si detector. Evidently, the temporal response of the device is similar to that of the Si detector. While this does not provide the actual time response of the device, it provides an upper limit of ~100 ns on the time response showing that the device is fast enough for most practical purposes.

4. QWIP characterization

The second portion of the device includes the QWIP. Here again, we grew a stand alone QWIP structure, fabricated a standard mesa structure and characterized its performances. The dark current, at different temperatures, is shown in Fig. 8. The dark characteristic measured at

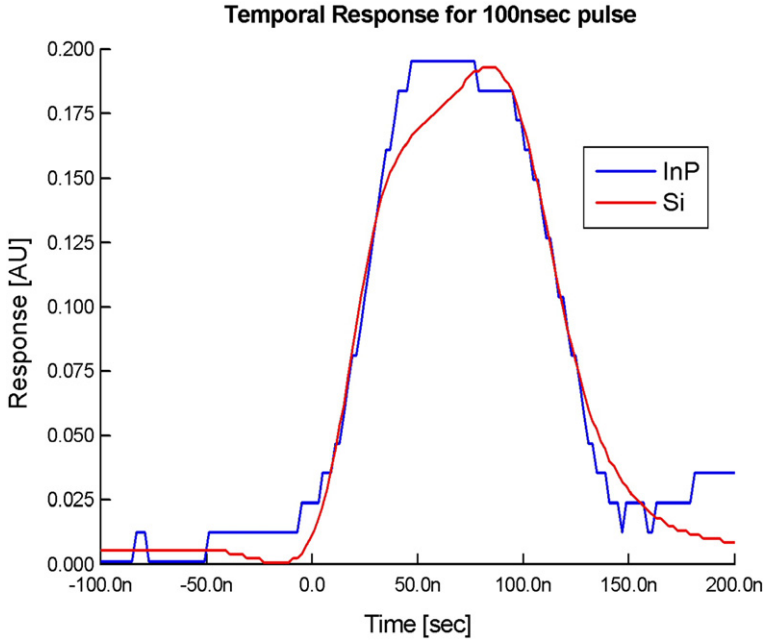

Fig. 7. Temporal response of the device compared with fast Si detector.

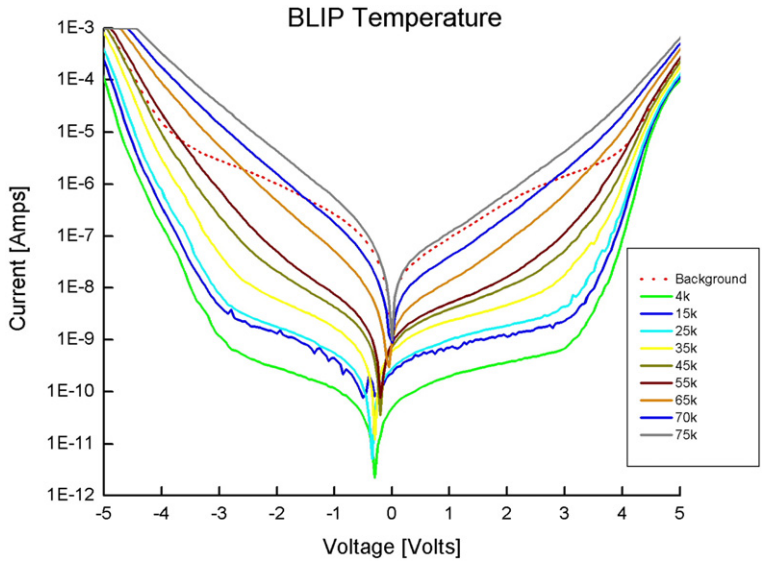

Fig. 8. BLIP temperature of the QWIP device. Solid lines – dark current at different temperatures, dashed line – background current at 14 K.

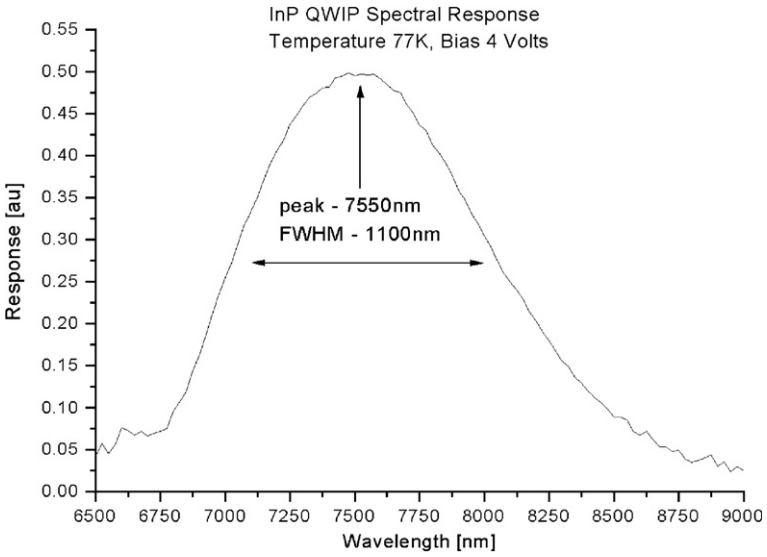

Fig. 9. Spectral response of the QWIP.

77 K is typical for InP based QWIPs [5]. In order to find the BLIP conditions, we have also measured the background current (dashed line in Fig. 8) at low temperatures (14 K). As can be seen, the BLIP temperature of the device at a bias voltage of ~3 V is about ~70 K, similar to the reports on similar InP based QWIPs [6]. The spectral response of the device is shown in Fig. 9. As can be seen the peak response is at about 7.6 μm, which would require an improved design as for imaging applications the peak should be red-shifted to longer wavelengths [7]. The FWHM of the response is fairly narrow, about ~1.1 μm. This could be an indication that the intersubband optical transitions are in between bound states (bound to bound state transitions in the QW).

5. Conclusions

We have demonstrated the concept of a second generation, two color IR imager that is based on monolithic integration of lattice-matched InP/InGaAs HBT and QWIP. This imager can be used for simultaneous imaging in the SWIR and the LWIR atmospheric windows. We have fabricated and characterized two InP/InGaAs structures of HBT and QWIP, showing that the basic concepts of the integrated device can be implemented in this material's system. The HBT detector showed a broad spectral response suitable for SWIR imaging applications together with very high sensitivity, low-noise and large photoconductive gain. The time response has been found to be better than 100 ns.

This device can be used for various applications, for example: applications where both active and passive imaging are required, a combination of thermal imaging with laser gated imaging and a 3D imaging system by combining thermal imaging with an array of range finders. The high sensitivity of the device, its wide bandwidth together with the simplicity of the fabrication process is expected to provide a cost effective product for complicated systems.

References

[1] N. Cohen et al., Infrared Physics Technology 47 (2005) 43–52.
[2] S.M. Sze, Physics of Semiconductors Devices, Wiley Interscience, 1969.
[3] J.C. Campbell, Phototransistors for Lightwave Communications at Semiconductors and Semimetals, vol. 22, Part D, Academic Press, London, 1985.
[4] J.C. Campbel et al., IEEE Journal of Quantum Electronics 19 (1983) 1134.
[5] J. Hasnain et al., Applied Physics Letters 57 (1990) 608.
[6] O.O. Cellek et al., IEEE Journal of Quantum Electronics 41 (2005) 980.
[7] B.F. Levine et al., Applied Physics Letters 53 (1988) 296.